Applied Geography 62 (2015) 377–390

Contents lists available at ScienceDirect

Applied Geography

journal homepage: www.elsevier.com/locate/apgeog

Mapping abandoned agricultural land in Kyzyl-Orda, Kazakhstan using satellite remote sensing

Fabian Löw [a, *], Elisabeth Fliemann [a], Iskandar Abdullaev [b], Christopher Conrad [a], John P.A. Lamers [c]

[a] Department of Remote Sensing, Würzburg University, Am Hubland, 97074 Würzburg, Germany
[b] CAREC, Almaty, Kazakhstan
[c] University of Bonn, Germany

ARTICLE INFO

Article history:
Received 7 March 2015
Received in revised form
25 May 2015
Accepted 25 May 2015
Available online

Keywords:
Abandoned cropland mapping
Central Asia
Aral sea
Land use trajectories
Decision fusion
Time-series

ABSTRACT

In many regions worldwide, cropland abandonment is growing, which has strong and known environmental and socio-economic consequences. Yet, spatially explicit information on the spatial pattern of abandonment is sparse, particularly in post-Soviet countries of Central Asia. When thriving reaching for key Millennium Development Goals such as food security and poverty reduction, the issue of cropland abandonment is critical and therefore must be monitored and limited, or land use transformed into an alternative one. Central Asia experienced large changes of its agricultural system after the collapse of the Soviet Union in 1991. Land degradation, which started already before independence, and cropland abandonment is growing in extent, but their spatial pattern remains ill-understood. The objective of this study was to map and analyse agricultural land use in the irrigated areas of Kyzyl-Orda, southern Kazakhstan, Central Asia. For mapping land use and identifying abandoned agricultural land, an object-based classification approach was applied. Random forest (RF) and support vector machines (SVM) algorithms permitted classifying Landsat and RapidEye data from 2009 to 2014. Overlaying these maps with information about irrigated land parcels, installed during the Soviet period, allowed indicating abandoned fields. Fusing the results of the two approaches, RF and SVM, resulted in classification accuracies of up to 97%. This was statistically significantly higher than with RF or SVM alone. Through the analysis of the land use trajectories, abandoned agricultural fields and a clear indication of abandoned land were identified on almost 50% of all fields in Kyzyl-Orda with an accuracy of approximately 80%. The outputs of this study may provide valuable information for planners, policy- and decision-makers to support better-informed decision-making like reducing possible environmental impacts of land abandonment, or identifying areas for sustainable intensification or re-cultivation.

1. Introduction

Agricultural production has increased worldwide, due to a combination of cropland expansion and an intensification of crop production on existing croplands (Foley et al., 2011; Lambin & Meyfroidt, 2011). Yet, concurrently, changing ecological, socio-economic, and political conditions, which triggered change in management practices, have also triggered cropland abandonment (Lambin & Geist, 2006). Outstanding examples of such conversions of agricultural land is seen after the collapse of the socialist governance structures in former Soviet Union countries, which in turn has lead to substantially declined agricultural production (Glantz, 2009; Létolle & Mainguet, 1996). Since independence in 1991, ca. 26 Million hectares farmland have been abandoned in Russia, Belarus, parts of Ukraine, and Kazakhstan (Lambin & Meyfroidt, 2011) and other former Soviet Union countries (Müller, Kuemmerle, Rusu, & Griffiths, 2009), although re-cultivation of abandoned land has partly occurred as well (Stefanski, Chaskovskyy, & Waske, 2014). Without restoration, abandonment cropland is linked to a particular set of problems, including landscape degradation, increased risk of erosion (Power, 2010). Yet, spatial and temporal patterns of cropland abandonment, especially in the former Soviet Union countries but in other parts of the world as well, remain ill-understood (Kuemmerle et al., 2013).

* Corresponding author.
E-mail address: fabian.loew@uni-wuerzburg.de (F. Löw).

http://dx.doi.org/10.1016/j.apgeog.2015.05.009
0143-6228/

Nevertheless, when thriving for global food security and reaching for key Millennium Development Goals such as food security and poverty reduction (www.un.org/millenniumgoals, last access 01-Mar 2015), cropland abandonment should be monitored, limited, or counterbalanced through a transformation into an alternative land use such as pasture.

Since abandoned cropland is often characterized by alterations in the surface conditions, for instance type and density of the vegetation cover, theoretically satellite remote sensing can support its mapping (Alcantara, Kuemmerle, Prishchepov, & Radeloff, 2012; Prishchepov, Radeloff, Dubinin, & Alcantara, 2012a, b; Stefanski et al., 2014). However, practically this is a challenging task because cropland abandonment is not characterized by a universal, fixed pattern (Lambin & Meyfroidt, 2011), that can easily be detected by satellite images. Whether or not abandoned cropland can be detected depends e.g. on the magnitude and duration of the alterations in land surface conditions due to land abolishment. Basically, abandoned cropland has been mapped either (i) through trend analysis, based on satellite time series of spectral indices such as the normalized difference vegetation index (NDVI), or (ii) by post-classification analysis of land cover trajectories (LCT). Trend analysis guided by the assumption that cropland abandonment results in decreasing trends of vegetation biomass, which can be identified in the satellite time series (De Beurs, Wright, & Henebry, 2009). However, a decreasing vegetation density can have many causes aside cropland abandonment, for instances long-term changes in agriculture towards other crop varieties. Furthermore, cropland abandonment may even trigger an increased NDVI due to a succession of weeds, grasses, and eventually shrubs or trees (Beurs, 2004). Hence, trend attribution, i.e. the assignment whether or not the detected trends actually relate to cropland abandonment, remains a challenging task (De Beurs et al., 2009; Wright, de Beurs, & Henebry, 2012). Further, a potential drawback of sensors like MODIS (250 m) or AVHRR (1000 m) is the pixel size. In many agricultural regions the pixel size can be of the same order of magnitude as the field size, which often results in misclassification (Löw & Duveiller, 2014; Ozdogan & Woodcock, 2006), whilst crop specific growth monitoring can even become impossible (Duveiller & Defourny, 2010).

The LCT approach assumes that specific temporal sequences (trajectories) of land cover and land use classes, which are distinct from actively used fields, can be used to identify certain stages of the agricultural land like fallow periods (c.f. Verburg, Schot, Dijst, & Veldkamp, 2004) including cropland abandonment (Estel et al., 2015; Peterson & Aunap, 1998; Prishchepov et al., 2012a, b). Usually, images from at least two different years are classified and compared. Although preliminary findings of the LCT approach were assessed as promising (Prishchepov et al., 2012a, b; Stefanski et al., 2014), the same studies revealed various, major challenges. First, LCT requires the collection of multiple images during one and the same growing season and for several years. Multi-seasonal images are important to capture accurately the different phenological stages, i.e. the beginning, middle and end of the growing season (Conrad et al., 2014; Löw, Michel, Dech, & Conrad, 2013). Multi-annual images are necessary to distinguish long-term from short-term changes and thus disclosing changes due to management intensities and accompanied perennial developments (Stefanski et al., 2014). But the frequency of multi-seasonal images is sometimes limited, for instance due to cloud cover or haze, which may negatively impact the quality of agricultural abandonment mapping using LCT (Fliemann, Löw, & Conrad, 2014; Prishchepov et al., 2012a, b). Also the number of consecutive years used for LCT influences results (Martinez-Casasnovas, Martín-Montero, & Auxiliadora Casterad, 2005). Hence, the choice of the multiple years to classify land use and detect abandoned cropland is crucial (Alcantara et al., 2012). However, in some parts of the world, suitable archives of satellite images are simply not available. For instance, Landsat images for the 1990s and beginning of 2000s are rare for many parts of Central Asia (CA) and other regions of the former Soviet Union, if existent at all (Prishchepov et al., 2012a, b). Further, complex crop rotation patterns, for instance those that include multi-annual fallow periods, renders the application of bi-annual LCT complicated, in particular when specific land uses have surface properties similar to abandoned fields (Alcantara et al., 2012; Prishchepov et al., 2012a, b). Misclassifications or misinterpretation of the results in turn could lead to false detection of changes (Foody, 2010). One alternative advocates the classification of a series of consecutive years, rather than years further apart in time and to analyse the corresponding LCT. However, studies actually providing evidence whether or not LCT, based on land use maps from consecutive years, is a reliable means for identifying abandoned cropland, are lacking still.

Beside the availability of adequate image data for all relevant time periods and adequate change detection approaches, the use of an accurate classifier algorithms is critical. The individual maps must be very accurate because uncertainty in the maps will reduce the reliability of land cover change analysis (Burnicki, Brown, & Goovaerts, 2007; Cockx, Van de Voorde, & Canters, 2014). Best classification accuracies in land cover classification are usually obtained with non-parametric machine learning algorithms like random forest (RF) (Pal, 2005; Waske & Braun, 2009) or support vector machines (SVM) (Huang, Davis, & Townshend, 2002; Pal & Mather, 2005). Both algorithms do not rely on statistical assumptions on the input data like normal distribution and are well suited to classify multi-temporal and multi-sensor data (Loosvelt, Peters, & Skriver, 2012; Waske & van der Linden, 2008). In the scope of agricultural land abandonment mapping, these algorithms gave already accurate results (Alcantara et al., 2012; Estel et al., 2015; Prishchepov et al., 2012a, b). Other approaches have combined the outputs of several classifier algorithms, usually referred to as a decision fusion approach. Recent studies illustrated a significant increase in classification accuracy when using a decision fusion (Fauvel, Chanussot, & Benediktsson, 2006; Waske, van der Linden, Benediktsson, Rabe, & Hostert, 2010), even though a significant increase is not warranted (Foody, Boyd, & Sanchez-Hernandez, 2007; Jeon & Landgrebe, 1999).

In comparison with other ex-Soviet Union countries (Alcantara et al., 2012; Baumann et al., 2011; Kuemmerle & Griffiths, 2009; Kuemmerle et al., 2008; Stefanski et al., 2014) and other regions worldwide (Falcucci, Maiorano, & Boitani, 2006; Park & Egbert, 2008), only few studies map abandoned cropland in CA (Akramkhanov & Vlek, 2012; De Beurs, Henebry, & Debeurs, 2004). In Kazakhstan, which is the largest producer of wheat and rice in the region and the third largest producer of cotton lint in CA (FAO, 2015), the causes of cropland abandonment and the spatial patterns of abandoned cropland are largely ill-understood (Anderson & Swinnen, 2008). Remote sensing could contribute in providing such key information needed to support policy and decision-makers, or planners in reducing possible environmental impacts of cropland abandonment, or identifying areas for sustainable intensification or re-cultivation and alternative land use practices (Dregne, 2002).

Therefore, the suitability of satellite remote sensing to detect abandoned cropland and to monitor related alterations in surface conditions was investigated in Kyzyl-Orda, southern Kazakhstan. An object-based (Blaschke, 2010) decision fusion approach needed to be designed to classify medium-resolution Landsat and RapidEye images, and to create annual maps of agricultural land use. Using a field cadastre database and satellite images for 2009–2014, the analysis focussed on cropland previously used for crop cultivation.

In doing so, change detection was combined with a detailed LCT analysis from post-Soviet times. The overall focus of this study was to (i) assess the potential of decision-fusion in comparison with non-parametric classifier algorithms to create an accurate archive of land use maps, (ii) to analyse LCT and identify thus abandoned cropland at the object-level, and to (iii) analyse the spatial pattern of abandoned agricultural land.

2. Study area

The study site in Kyzyl-Orda (Fig. 1) covers about 19.800 km^2. It is located 115 m above sea level in a flat lowland region at the lower reach of the Syrdarya, approximately 350 km east of the former Aral Sea shorelines. The climate is arid and continental, with on average 149 mm annual precipitation that mainly falls in spring and late autumn. The dominant soil types are *Eutric Fluvisols* in the flood plains of the Syrdarya river (fluvial deposits, suitable for agriculture), *Eutric Gleysols* (soils saturated with groundwater unsuitable for cropping unless adequately drained), *Eutric Histosols* (ill-suitable for cropping due to a poor drainage and often low chemical fertility, but can be cropped under adequate drainage), and *Calcic* and *Takyric Yermosols* (desert sand plain soils, with heavy texture and surfaces cracks in dry condition and surface crust or, in case of calcic, with a strong accumulation of calcium carbonate, ill-suitable for cropping) (FAO-UNESCO, 1974; IUSS Working Group WRB, 2014). The fringe area between the alluvial plain of the Syrdarya and the Kyzyl-Kum desert is characterized by (shifting) dunes, which are unattractive for agriculture, due to their low organic matter content and mobile surfaces (FAO-UNESCO, 1974).

Next to the natural riverine vegetation near the Syrdarya, open shrublands and patches of reed areas dominate the landscape in Kyzyl-Orda. Rice and alfalfa cultivation is dominating with typical seasonal cropping calendars suitable for land use classification. In spring (April–May) of each year, rice fields are partly covered with bare soil or, in case of early maturing varieties, already watered, whilst shrubs are already greening. Each summer (June–August), fields are either watered (e.g. late maturing rice varieties) or already greening due to the cultivation of early maturing rice varieties, alfalfa, or other herbaceous vegetation. Between September and the beginning of October, vegetation is not yet dormant, but rice or alfalfa is usually harvested and soil tilling usually toy takes place. Rice and alfalfa cultivation are part of a crop rotation with a distinct temporal pattern (Funakawa, Suzuki, Karbozova, Kosaki, & Ishida, 2000). After two years of rice cultivation, the fields are left fallow for three consecutive years leaving room and for the growth of herbaceous vegetation and legume crops, in particular alfalfa, is grown for up to three consecutive years. Next, other crops (such as wheat and vegetables) are grown for two consecutive years before rice is cultivated again for two years. This rotation has since 2009 become mandatory in Kyzyl-Orda oblast since 2009 as an imposed means to conserve and regenerate soil fertility (oral communication with Dr. Ulikbanuli Nurlibai, vice-director of the Rice Institute in Kyzyl-Orda). The same crop is grown on adjacent fields, which together exceed the area of between 500 × 500 m and 1000 × 1000 m (25–100 ha). The areas between such blocks of fields are usually covered with sparse shrub or, to a lesser extent, herbaceous vegetation and bare soil.

The expansion of agricultural land in Kazakhstan during the Soviet epoch was accompanied with widespread soil salinization, which has remained as one of the major challenges (Funakawa et al., 2000). Aside from a wide spread soil salinization in Kazakhstan (cf. Funakawa et al., 2000), soil degradation is enhanced through the loss of soil organic matter, which has impacted 30–40% of the soils of the irrigated areas in Kyzyl Orda (Ibraeva, Otarov, Wiłkomirski, & Suska-malawska, 2010). Shrub encroachment usually occurs three to five years after cropland abandonment, probably with faster shrub advancement on well-drained and formerly ploughed fields. Abandoned fields remain devoid of any vegetation once suffering strong soil salinization.

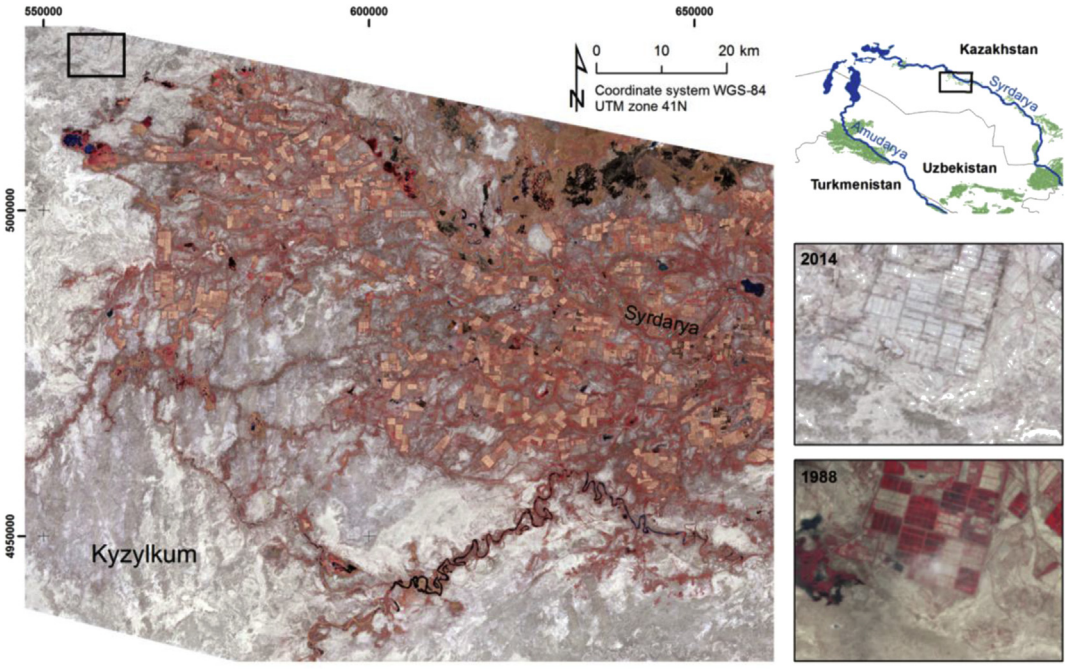

Fig. 1. Landsat image of the study area in April 2014. Landsat images are displayed in false-colour band combination 4-3-2, vegetation appears in red colours, water in dark blue and black colours. Small image subsets (right) illustrate changes in vegetation cover between 1988 (bottom) and 2014 (top). (For interpretation of the references to colour in this figure legend, the reader is referred to the web version of this article.)

3. Materials

3.1. Satellite data and pre-processing

Cropland abandonment through the LCT analysis for 2009–2014 was assessed within the boundaries of all land parcels that had actively been used during the Soviet era. For land use classification, Landsat images (30 m spatial resolution) were downloaded from the United States Geological Survey (USGS; http://earthexplorer.usgs.gov/). The Landsat tile 158/029 was selected, because of an abundance of abandoned fields, field accessibility for collecting ground reference data and comparatively good data availability (e.g. cloud cover of the images was limited to 10%, clouds did not cover agricultural fields).

In 2011, the Landsat data was supplemented with RapidEye level 1B images (6.5 m spatial resolution), which were made available by RESA to fill gaps in the Landsat time series. Cloud free images were selected during April–October in each year (Table 1). For entire 2012, no images were available owing to the malfunction of Landsat-5 TM, whilst Landsat-8 was launched in 2013 only. Other high-resolution images like SPOT were not available in this study to further compensate for gaps in the time series.

Several monthly images were selected per year to capture the different phenological stages of the vegetation for each year (Table 1). The images were co-registered to two high-resolution SPOT-5 images (2.5 m) from 2011, which had been geo-corrected using ground control points sampled in 2011. A nearest-neighbour transformation of all Landsat and RapidEye images to the Universal Trans Mercator (UTM) reference projection (WGS84 datum) resulted in acceptable sub-pixel accuracies (RMSE $\leq$ 0.9 pixels) for all images. All Images used were atmospherically corrected using the ATCOR-2 module for flat terrain (Richter, 2011) to retrieve the "top-of-canopy" reflectance. Haze and dust, which was most probably caused due to the proximity of the region to the Kyzyl-Kum desert, were removed with ATCOR. Landsat-5 bands 1–5 plus 7, and Landsat-8 bands 2–7 were used to achieve as much as possible the same spectral information as input for the classification.

Table 1
Landsat images used for classification. LS5 = Landsat-5 TM; LS8 = Landsat-8 OLI; RE = RapidEye. Six bands of LS5 were used: blue (450–520 nm), green (520–600 nm), red (630–690 nm), NIR (760–900 nm), SWIR1 (1.550–1.750 nm), SWIR2 (2.080–2.350 nm). Six bands of LS8 were used: blue (450–510 nm), green (530–590 nm), red (60–670 nm), NIR (850–880 nm), SWIR1 (1.570–1.650 nm), SWIR2 (2.110–2.290 nm). All five RE bands were used: blue (440–510 nm), green (520–590 nm), red (630–685 nm), red edge (690–730 nm), and near infrared (NIR, 760–850 nm).

ID	Year	Month	Day	Dataset
1	2009	May	22	LS5
2		Jun	23	LS5
3		Jul	09	LS5
4		Sep	11	LS5
5		Sep	27	LS5
6		Oct	13	LS5
7	2010	Apr	23	LS5
8		June	26	LS5
9		Jul	28	LS5
10		Aug	29	LS5
11		Sep	30	LS5
12	2011	Apr	10	LS5
13		May	12	RE
14		Jul	02/03	RE
15		Aug	13/16/17	RE
16		Sep	17/22/24	RE
17		Oct	03	LS5
18	2013	Apr	15	LS8
19		May	17	LS8
20		Jun	18	LS8
21		Sep	06	LS8
22		Sep	22	LS8
23	2014	Apr	18	LS8
24		May	04	LS8
25		May	20	LS8
26		Jun	05	LS8
27		Jul	23	LS8
28		Aug	08	LS8
29		Sep	09	LS8

3.2. Vector data of agricultural fields

Given the objective to map abandoned agricultural fields and due to the absence of an appropriate number of satellite images from the Soviet Union time, a vector database needed to be created that contained all formerly used field objects in the study area. Objects were digitized on-screen using the high-resolution SPOT images (2.5 m) of 2011 and GoogleEarth. By doing so, all previously used field parcels could be identified owing to the spoors of the canal infrastructure, which are still visible in these data sets. This permitted demarcating field boundaries designed during the Soviet Union (see Fig. 1, small image subset from 2014). Altogether, digitization resulted in 66,281 field objects, corresponding to 209,874.45 ha (circa 11.5% of the study area), with an average field size of 3.44 ha and a median field size of 2.34 ha.

For the image classification, mean and standard deviation values of several vegetation indices (VI) were calculated for each object and acquisition date: NDVI (Rouse, Haas, Schell, & Deering, 1974), the tasselled cap indices greenness, wetness and brightness based on Landsat (Huang, Wylie, Yang, Homer, & Zylstra, 2002; Kauth & Thomas, 1976) and RapidEye (Schönert, Weichelt, Zillmann, & Jürgens, 2014), the enhanced vegetation index (EVI) (Huete, Didan, Miura, Gao, & Ferreira, 2002), and the spectral bands of Landsat and RapidEye (Table 1). With six acquisition dates of Landsat, this resulted in 132 spectral-temporal features per object.

3.3. Classification reference data

In 2011, an extensive ground campaign have been conducted to collect reference data for the training and validation of the classifier algorithms, which represented an expert-based assignment of reference field objects (polygons) to certain land-use classes. Crop type and plant development status (i.e. growing stage, stand homogeneity, plant height), had been recorded with a GPS camera with a geo-location accuracy of 2–3 m. Only fields with homogeneous growing conditions, covered exclusively with one land use type, were used as reference fields. In the other years, all reference samples had been collected by visual interpretation of Landsat images and a comparison of the NDVI signatures of the training samples from 2011. Reference data fields had been selected at minimal 750 m apart to reduce spatial auto-correlation, i.e. sampling nearby fields of the same class was avoided, as this would likely add redundant information for the classifier algorithm training. The reference data sets represent five classes: (Fig. 2): rice fields (Fig. 2a), herbaceous vegetation (e.g. sparse herbaceous vegetation or alfalfa as feed crop, Fig. 2b), shrublands (mostly *Tamarix* sp., Fig. 2c), bare soils (i.e. without vegetation, Fig. 2d), and water (e.g. permanently flooded fields). Following a random sampling scheme, between 532 and 676 samples had been collected each year (Table 2). In 2011, when samples were collected on the ground, a pure random sampling scheme had to be adjusted due to restrictions in access to fields (bad road conditions, missing permission by farmers, partly broken bridges).

Fig. 2. Agricultural land use categories sampled in the Kyzyl-Orda oblast in southern Kazakhstan. A: Rice field. B: Herbaceous vegetation (alfalfa). C: Abandoned field with dense shrub cover. D: Abandoned field with bare soil cover. E: Water.

Table 2
Number (N) of reference fields for land use classification.

Year	N	Bare soil	Herb. vegetation	Rice	Shrubland	Water
2009	532	102	104	194	94	38
2010	584	104	132	176	102	70
2011	676	138	178	200	98	62
2013	562	106	102	170	104	80
2014	544	118	102	166	110	48

4. Methods

The identification and mapping of abandoned agricultural land, through object-based classification of satellite image time series for 2009–2014, followed a step-wise approach: (i) generating a vector data base of all ever used fields in the study region, (ii) generating land use maps for 2009–2014, (ii) creating a multi-year land use archive for each field object and (iii) analysing the LCT in relation to the vector database representing all, ever-used agricultural field objects (Fig. 3).

4.1. Object based classification

Land use maps had been created for each year by supervised image classification of annual image stacks from Landsat (and RapidEye in 2011) that consisted of 5–6 images each (Table 1). Since land use classifications are most accurate when using non-parametric machine learning algorithms (Mountrakis, Im, & Ogole, 2011; Waske & Braun, 2009), random forests (RFs) (Breiman, 2001) and support vector machines (SVMs) (Cortes & Vapnik, 1995) had been selected. Both classifiers had performed comparatively well in classifying complex data sets like optical or radar satellite image time series (Huang et al., 2002a; Löw et al., 2013; Waske & Braun, 2009). Yet, since errors in land use classification may translate into spurious change detection results (Foody, 2010), the outputs from RF and SVM were fused to enhance classification accuracy.

Model building, tuning, and accuracy assessments have been completed with the software R (R Development Core Team, 2014). First, the reference data of each year had been split into two independent data sets by randomly selecting 50% of the samples for training and testing, respectively. The number of features m_{try} to split the nodes in the trees (Breiman & Cutler, 2007) was set to the square root of the total number of input features (Gislason, Benediktsson, & Sveinsson, 2006). The final number of trees in the RF ensemble was set to 300. Training of the SVM included choosing the kernel parameter γ and the regularization parameter C, where γ determined the width of the kernel, and C controlled the

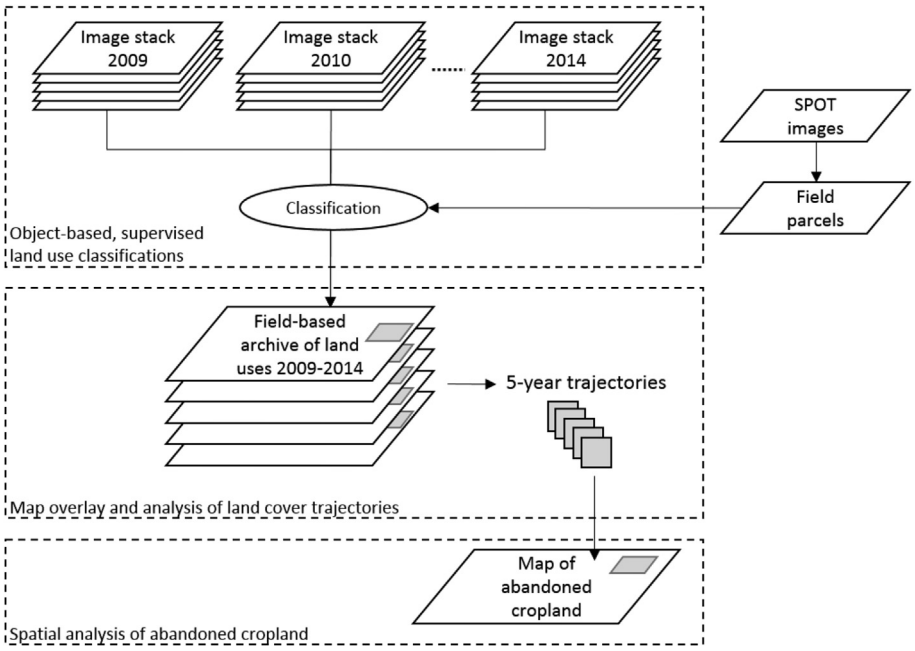

Fig. 3. Flowchart depicting the major steps to detect abandoned cropland.

penalty associated with misclassified training samples (Burges, 1998). Further, C and γ had been tuned by using a systematic grid search in 2-D space that was spanned by γ and C. The range of γ was [0.00125, 10], the range of C was finally set to [1, 200]. The widely used radial basis function (RBF) kernel was selected. The data space was normalized to a common scale [0, 1].

The RF and SVM models were trained and applied on randomly selected feature subsets from the input data (see Section 3.2), which comprise 50% of the total number of spectral-temporal features each. In doing so, multiple realizations of land use maps were generated, each based on a randomly selected subset of features. In this study, 50 random draws of feature subsets had been realized in each year separately. This resulted in 100 land use classifications per object (50 by RF, and 50 by SVM), enabling to create multiple class labels for each object. Random feature selection has previously been reported to enhance classification accuracy (Ho, 1998; Waske et al., 2010) and was here further enhanced by selecting two different algorithms, RF and SVM. Finally, a majority voting was applied on the classification outputs from RF and SVM to assign the final class to the corresponding field object.

Classification accuracy was evaluated with confusion matrices based on independent test sets (Congalton, 1991). Overall accuracy was calculated as a percentage of correctly classified test objects. The accuracies achieved by the different classification approaches were reported using exact 95% confidence intervals. When dealing with a normal distribution or when a large sample is disposed, the confidence interval of the difference (inequality) in overall accuracy values between two classifier algorithms can be given as:

$$p_1 - p_0 \pm z_{a/2} SE_{p_1 - p_0} \tag{1}$$

where SE_{p1-p0} is the standard error of the difference between two estimated proportions with $z = 1.96$ and $\alpha = 0.05$. p_1 and p_0 are the proportions of correctly classified tests samples of the two classifiers under comparison. Using confidence intervals allows for revealing more information about the disparity in the classification accuracy values compared (Foody, 2009). The McNemar test, designed to evaluate differences among proportions that are not independent and that have been widely used in remote sensing (Foody, 2009), was used to evaluate the statistical significance of the observed differences in the classification accuracies. All pairwise combinations of any two maps using the same validation dataset are compared. The Z-scores have been used to test if two classifications significantly differ at $\alpha = 0.05$ if $z = |1$. The z-score was calculated by normalizing the differences in the off diagonal of the cross-tabulation as:

$$z^2 = \frac{(n_{10} - n_{01})^2}{n_{10} + n_{01}}. \tag{2}$$

Next to the overall accuracy, a class-wise measure of accuracy, was employed for each class i under investigation, defined as the number of correctly classified test samples belonging to a class i.

4.2. Identification of abandoned cropland

The temporal sequences of land uses between 2009 and 2014 were assessed for identifying abandoned cropland within the field vector layer (Section 3.2). The following major trajectories were assumed indicative for cropland abandonment: (i) five year lasting cover of shrubs or bare soil; (ii) transitions of bare soil to herbaceous vegetation and (iii) transitions from herbaceous vegetation to shrub (both assumed to indicate different stages of an on-going succession of vegetation on abandoned fields). Other land-use change processes that lead to the loss of agricultural land, such as urban development, have been excluded. Urban areas were digitized on-screen based in GoogleEarth in 2014.

Two major trajectories represented actively used fields: (i) permanent rice cultivation and (ii) multiple changes of rice and herbaceous vegetation, which is assumed to be at the core of the crop rotation systems in Kyzyl Orda (cf. Section 2). Due to the data gap in 2012, a gapless compliance with the official recommendation could not be completed. The remaining trajectories have been summarized under the class “Others”, including, for example, multiple changes of bare soil, herbaceous vegetation, and shrubs, and the status of such field was assumed to be uncertain.

The accuracy of the approach to identify abandoned cropland was validated through a second independent test set, which contained 250 field samples for two classes: abandoned fields and actively used fields. Following the same sampling procedure as for the land use, classification samples (see Section 3.3), additional reference samples were selected on-screen in Google Earth in the year 2014. These samples contained different stages of cropland abandonment, i.e. bare soils, herbaceous vegetation, and shrubland. Based on the second test data set it was also investigated how long the observation period, i.e. the number of consecutive years, must be to obtain reliable results through the proposed LCT analysis. The LCT analysis, based on multiple years, was further compared to single year assessments of land abandonment, where for instance shrubland and bare soils were assumed as abandoned land and rice fields as active land.

4.3. Analysis of spatial pattern of land abandonment

To further explore the spatial pattern of land abandonment, the final classification result was overlaid with a number of spatial indicators related to the marginality of farming (across gradients of soil marginality). These were finally analysed with regard to their possible impact on the observed spatial pattern of abandoned fields.

5. Results

5.1. Accuracy of object-based classification

The accuracy assessment, based on the comparison of the classification results with the test set data, revealed that RF and SVM performed accurate in all years (Table 3). The overall accuracy of both algorithms ranged from 0.843 to 0.908, but the RF was slightly more accurate than SVM in four out of five years. However, given the large overlap in the 95% confidence intervals for overall accuracy (Table 3), the two algorithms scored within the same range of accuracy.

The fusion approach gave significantly (i.e. at the 95% confidence level) more accurate results than that with RF or SVM alone. This is also revealed by the non-overlapping confidence intervals of the fusion on the one, and RF or SVM on the other site. Using decision fusion resulted in an increase in overall accuracy of up to 7%, compared to RF or SVM, with high overall accuracies in all years (0.936–0.979). With the fusion, the lowest overall accuracy occurred in 2009 and the highest overall accuracy was achieved in 2011 and 2014.

The classification based on the fusion approach gave a good separation of the five land use classes. The highest positive gain in class-wise accuracies was achieved for herbaceous vegetation and shrubs. Tables 4 and 5 exemplary shows the differences in class-wise accuracies in 2011, when ground reference data was available. Class-wise accuracies of the fusion approach were generally high between 2009 and 2014 (Table 6). Lowest class-wise accuracy was observed for herbaceous vegetation, which was mostly due to an ill-discrimination from shrubs. Highest class-wise accuracy was achieved for water and rice, most obviously due to the distinct spectral signature of water, including watered rice fields. Overall, the accurate five land use maps based on the fusion approach permitted thus consequently a reliable analysis of the envisaged change trajectories.

Table 4
Class-wise accuracies for random forest (RF), support vector machines (SVM) and decision fusion (FUS) in 2011.

Year	Herb. Vegetation	Rice	Shrubs	Bare soil	Water
RF	0.843	0.991	0.853	0.993	0.997
SVM	0.816	0.923	0.848	0.994	0.996
FUS	0.961	0.995	0.929	0.993	1.000

5.2. Accuracy of the LCT method for detecting cropland abandonment

After assessing the five single years, the LCTs were analysed to detect abandoned cropland. Based on the second test set, adding stepwise more years resulted in a statistical significantly better discrimination between abandoned and actively used fields (Fig. 4). The highest overall accuracy was therefore achieved when considering all land use maps (2009–2014), as evidenced by an overall accuracy of almost 0.799 (interval: 0.757–0.835). Any combination of two years gave worse results than the full data set (Fig. 4). For instance, when only 2013 and 2014 were compared, the accuracy amounted to 0.715 (interval: 0.678–0.758) only. Differences among the single years were marginal, with the exception of 2013, which was the least accurate (overall accuracy: 0.631, interval 0.586–0.674). The findings showed that 2011 was the most accurate single year (overall accuracy: 0.688, interval 0.647–0.723), most probably due to the availability of on-site reference data for this year. It must be noted that based on the observation period 2009–2014, the status of almost 15% of the fields still remained uncertain, i.e. these were characterized by not particularly investigated change classes, including implausible classes. These 15% fields were neither labelled “active” nor “abandoned”.

5.3. Analysis of land use trajectories

Herbaceous vegetation and rice fields as well as shrubs were the three dominant land use types (Fig. 5). Together they comprise over 86% of the total land area (averaged over the period 2009–2014).

A slight increase of shrubs was observed between 2009 and 2014 (Fig. 5), indicating a steady progress of shrub encroachment on abandoned fields. Shrubs covered approximately 25% of the observed fields in 2009 and 26% in 2014. Bare soils covered, on average, 13% of the fields between 2009 and 2014, whilst

Table 3
Overall accuracies (ACC) and lower (L95 CI) and upper (U95 CI) confidence intervals for random forest (RF), support vector machines (SVM) and decision fusions (FUS).

Year	RF			SVM			FUS		
	ACC	L95 CI	U95 CI	ACC	L95 CI	U95 CI	ACC	L95 CI	U95 CI
2009	0.843	0.825	0.859	0.880	0.863	0.897	0.936***	0.923	0.948
2010	0.908	0.895	0.921	0.897	0.883	0.910	0.963***	0.954	0.972
2011	0.906	0.882	0.907	0.884	0.860	0.905	0.976***	0.968	0.989
2013	0.902	0.888	0.915	0.897	0.882	0.911	0.971***	0.964	0.977
2014	0.905	0.893	0.916	0.899	0.883	0.914	0.979***	0.975	0.985

Note: Asterisks indicate the level of statistical significance between the fusion approach and the single best classifier algorithm: $0.10 > p > 0.05$: *, $0.05 > p > 0.01$: **, $0.01 > p > 0.001$: ***, according to the McNemar test.

Table 5
Confusion matrix for the decision fusion approach year 2011. Lower (L95 CI) and upper (U95 CI) confidence intervals of the overall accuracy are given.

Prediction						
Reference	Herb. vegetation	Rice	Shrubs	Bare soil	Water	Class-wise accuracy
Herb. vegetation	171	0	7	0	0	0.961
Rice	0	199	0	0	1	0.995
Shrubs	5	0	91	2	0	0.929
Bare soil	0	0	1	137	0	0.993
Water	0	0	0	0	62	1.000
Overall accuracy	0.976 (L95 CI: 0.968, U95 CI: 0.989)					

Table 6
Class-wise accuracies, overall accuracies (ACC), lower (L95 CI) and upper (U95 CI) confidence intervals for the decision fusion approach.

Year	Herb. vegetation	Rice	Shrubs	Bare soil	Water	ACC	L95 CI	U95 CI
2009	0.866	0.995	0.816	1.000	0.996	0.936	0.923	0.948
2010	0.903	0.993	0.933	0.994	0.995	0.963	0.954	0.972
2011	0.961	0.995	0.929	0.993	1.000	0.976	0.968	0.989
2013	0.989	0.981	0.928	0.951	0.998	0.971	0.964	0.977
2014	0.963	0.976	0.973	0.994	1.000	0.979	0.975	0.985

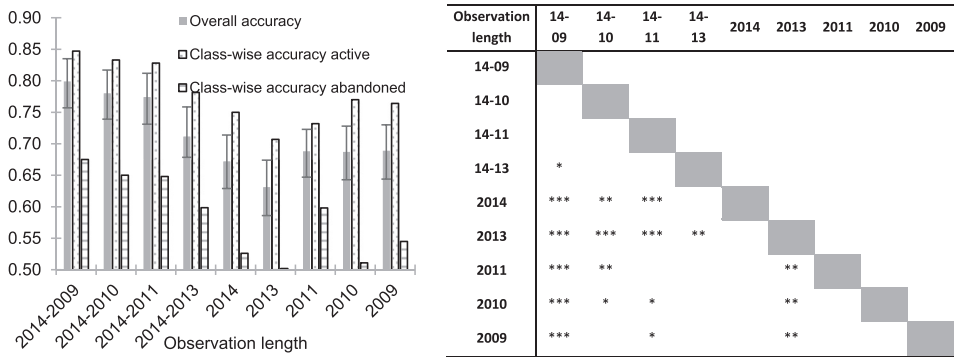

Fig. 4. Left: Overall accuracies of detecting abandoned cropland as a function of the length of the observation period (i.e. number of land use maps). Error-bars indicate the 95% confidence interval around the overall accuracy. Right: Statistical significance of the differences in accuracies among different models. Asterisks represent the threshold at which there is a significant difference at a p-value of $0.10 > p > 0.05$: *, $0.05 > p > 0.01$: **, $0.01 > p > 0.001$: ***, according to the McNemar test.

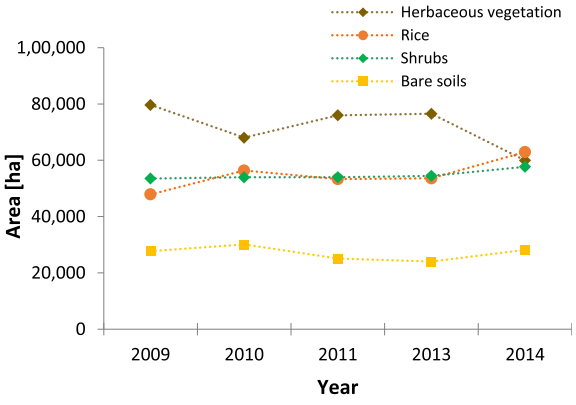

Fig. 5. Annual changes of area of five land use classes.

herbaceous vegetation covered the major part of the landscape (ca. 34%), followed by rice and shrubs (ca. 26%). Since rice and herbaceous vegetation are part of the cropping scheme in Kyzyl-Orda, the area shares of both were mutually dependent. The increase of fields with herbaceous vegetation between 2009 and 2014 nearly matched the decrease in the area of rice and partly by bare area. Water only covered a marginal part of the landscape (<1%).

5.4. Spatial pattern of abandoned cropland

The inner part of the study area, i.e. apart from the fringe to the Kyzyl-Kum desert, was predominantly used for rice cropping in rotation with herbaceous vegetation periods (Fig. 6). At the most remote parts, i.e. at the desert fringe, agricultural fields were permanently devoid of vegetation (i.e. five years bare soil). A zone that is characterized by transitions from bare soil to herbaceous vegetation, and further from herbaceous vegetation to shrubs was located between the desert fringe and the inner part of the agricultural area. Most of the actively used fields were located in the central part of the study area, where rice fields were aggregated to larger blocks, which is the typical pattern of cultivation in this region (section 2). In this inner part of the study area, abandoned fields that had been characterized by conversions of herbaceous vegetation to shrubs or five-year lasting shrub cover were intermixed, but without a clear spatial pattern. Further, LCT that could not be assigned to active or abandoned fields, are spread all over the inner parts of the agricultural area.

The LCT rate was almost 82%, which means that on 18% of the fields the same land use type was found over the entire observation period (Table 5). Moreover, roughly one third (ca. 32%) of the fields turned out to be cultivated with rice in rotation with herbaceous vegetation, indicating that these fields were actively being used between 2009 and 2014 while following a crop rotation consisting

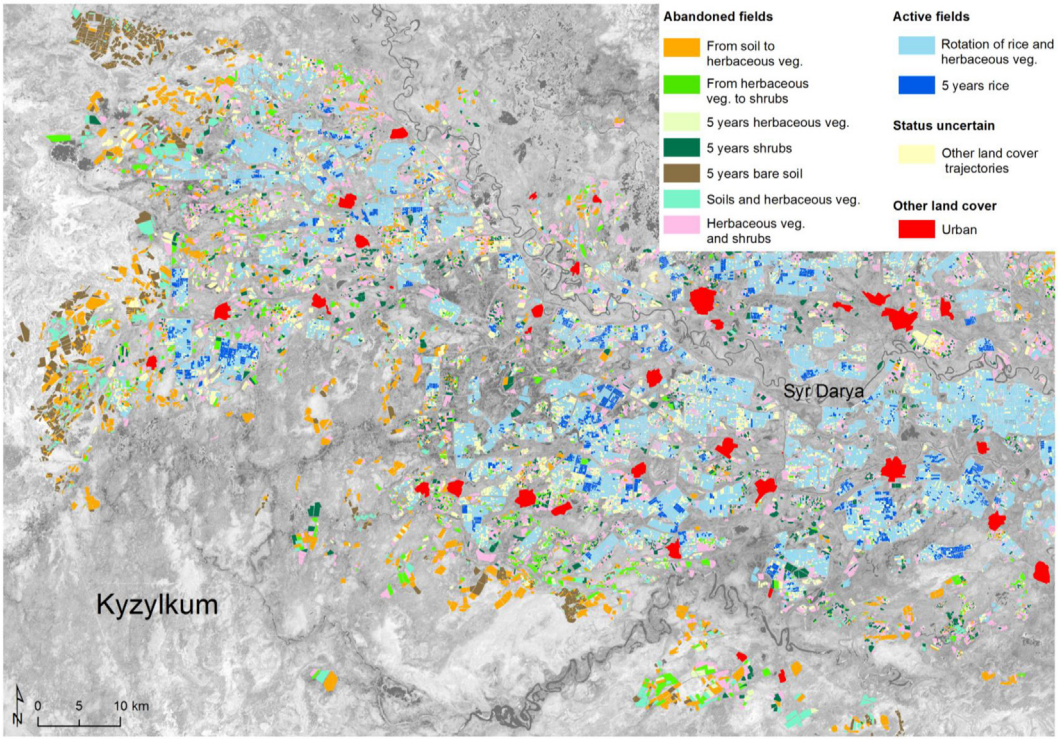

Fig. 6. Main multi-year land cover trajectories in Kyzyl-Orda, 2009–2014.

of 1–4 years of rice cultivation, in rotation with herbaceous vegetation. On ca. 5% of the agricultural land, mono-cropping sequences of rice were detected contradicting thus official recommendations, which stipulate a 2–3 year fallow period with alfalfa or other herbaceous vegetation after 1–4 years of rice cultivation. Conversions from bare soil to herbaceous vegetation (ca. 10%) and further from herbaceous vegetation to shrub (ca. 4%) indicated a re-establishment of vegetation on abandoned fields. Other combinations of herbaceous vegetation and shrubs constituted a large portion (ca. 18%). The quantitative analysis of the total abandonment revealed that almost 50% of the fields in Kyzyl-Orda had not actively been in use in 2014 (Table 7). About 15% of the fields were characterized by LCT that neither could be assigned to abandoned nor to actively used fields with certainty. Hence, their exact status remained uncertain.

To explore the spatial pattern of abandoned cropland, the final classification (Fig. 6) was overlaid with a soil map (Fig. 7). The majority of soils were classified as *Eutric Histosols* and *Takyric Yermosols* (section 2). As expected, abandoned fields dominated on soils of marginal fertility, e.g. *Takyric Yermosols* or dunes or shifting sands at the desert fringe. However, a large fraction of abandoned fields was found on *Eutric Histosols* also, which usually are intensively cultivated. Rice production in the study area occurs on various soil types, but for a large part on *Eutric Fluvisols* (approx. 25%) and *Eutric Histosols* (approx. 40%). A considerable part of the actively used fields were located on *Takyric Yermosols* (approx. 23%) whilst the fields on *Eutric Gleysols* were mostly abandoned or had an uncertain status. In comparison to the other soil types, relatively few fields (abandoned or active together) were found on *Eutric Fluvisols* despite their known suitability for agriculture (FAO-UNESCO, 1974; IUSS Working Group WRB, 2014).

6. Discussion

6.1. Field-based classification

Agricultural land use and land abandonment were monitored and analysed, based on satellite remote sensing. The first objective was to map and monitor land use in the period 2009–2014. As expected (Löw et al., 2013; Waske & Braun, 2009), the used

Table 7
Quantification of land abandonment and land use in Kyzyl-Orda, based on the land cover trajectory (LCT) analysis in the period 2009–2014.

Multiyear class	N fields	Area [ha]	Area [%]	Assumed status of fields
Rotation of herbaceous vegetation and rice	27,033	68,783.94	32.77	Active
Herbaceous vegetation and shrubs	13,293	38,649.78	18.42	Abandoned
Other LCT	9421	26,376.19	12.57	Uncertain
Soil to herbaceous vegetation	2964	21,581.74	10.28	Abandoned
5 years Shrubs	1062	12,001.67	5.72	Abandoned
5 years Rice	4639	11,131.79	5.30	Active
5 years bare Soil	1650	10,927.46	5.21	Abandoned
Herbaceous vegetation to shrubs	2501	9455.15	4.51	Abandoned
Soils and herbaceous vegetation	980	7119.29	3.39	Abandoned
5 years herbaceous vegetation	1309	3847.44	1.83	Uncertain
Total area:		209,874.45	100.00	

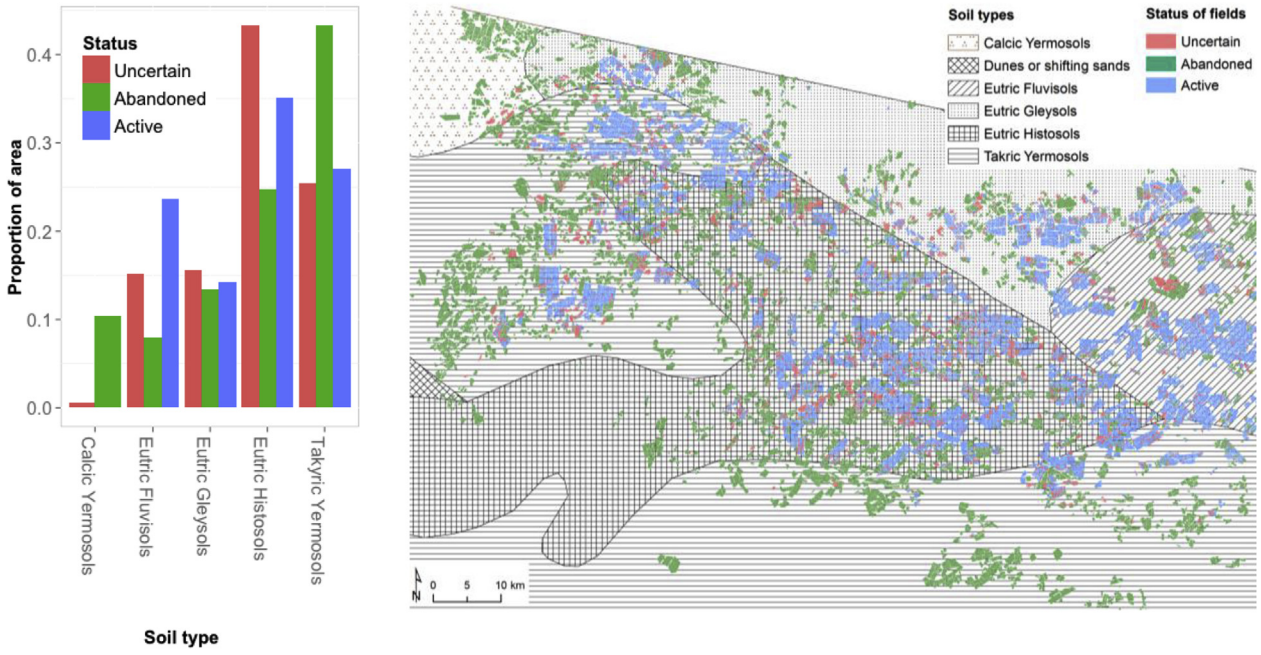

Fig. 7. Left: Area proportion of fields with different usage status across underlying soil types. Right: Spatial distribution of agricultural fields and soil types in Kyzyl-Orda.

classification algorithms performed at high accuracy levels, with overall accuracies ranging from 0.85 to 0.90. The present results together with those of others (Murakami, Ogawa, Ishitsuka, Kumagai, & Saito, 2001; De Wit & Clever 2004) investigating the benefit of multi-temporal, object-based classification of remote sensing data for accurately mapping crop distribution confirm, that an accurate land use classification is likely to increase when having a good temporal coverage of at least five observations per year (Table 1). The lowest overall accuracy occurred in 2009, the year when images for April and August were unavailable. Both months however are periods with a crucial phenological stage needed to discriminate between shrubs and herbaceous vegetation with similar phenology and avoiding a misclassification of herbaceous vegetation with beginning shrub encroachment. Despite some possible (multi) co-linearity in the data sets, no pre-selection of features was performed because RF and SVM were shown to be only affected when very small training data sets are used (Pal & Foody, 2010). In Loosvelt et al. (2012) the reduction of redundant features even lad to decreases in accuracy. Further, the random feature selection of the proposed fusion strategy contributed to reduction in redundant information.

Due to known challenges in distinguishing complex land cover types, a fusion strategy was employed to enhance the classification accuracy. Although both (RF and SVM) classifiers performed differently for land use classes, there was a large overlap in the 95% confidence intervals of the revealed overall accuracies. The achieved significant increase in accuracies through the fusion was most likely due to the complementary algorithms of RF and SVM, because they are based on different approaches. For instance, SVMs are based on a few relatively complex decision boundaries. In linear non-separable cases, the input data is transferred into a higher dimensional feature space (Hilbert space) that enabled the generation of a decision boundary that appeared nonlinear in the original feature space. In contrast, the RF approach is based on several single decision tree classifiers, which constructs many rather simple decision boundaries that are parallel to the feature axis. However, although the presented accuracy improvements by decision fusion are in accordance with previous findings (Licciardi et al., 2009; Waske & van der Linden, 2008), it should be noted as well that achieving higher accuracies with classifier fusion is not guaranteed (Foody et al., 2007; Giacco, Thiel, Pugliese, Scarpetta, & Marinaro, 2010). Nevertheless, the increased accuracy achieved by the decision fusion can be assessed beneficial for the subsequent LCT analysis and for the identification of abandoned cropland, which demanded highly accurate classifications at every year under investigation.

Still, and irrespective of the selected approach (RF, SVM, decision fusion), classes such as alfalfa and other herbaceous vegetation could not always be discriminated due to their spectral similarity and because both are subjected to irregular cutting operations during the growing season (Fig. 8). Therefore, they were kept merged into one class (herbaceous vegetation). The application of MODIS, with a high temporal revisit frequency, recurrently is a suitable alternative for a detailed crop mapping including alfalfa classes (Wardlow & Egbert, 2008). However, the relatively small field sizes and heterogeneous pattern of fields with herbaceous vegetation in Kyzyl-Orda are likely to give mixed signals in the coarser MODIS pixels, leading to reduced classification accuracies, as shown previously by Löw and Duveiller (2014) for a test site in Kyzyl-Orda. Other options for a better discrimination of vegetation types, i.e. the separation of alfalfa fields from natural herbaceous vegetation on abandoned fields, could be the use of hyperspectral (Waske et al., 2010) or SAR data. Schuster, Ali, Lohmann, Frick, and Förster (2011) demonstrated the ability of TerraSAR-X data for mapping swath events in grasslands, which could be useful to observe unregularly cutting events and hence to better distinguish alfalfa fields from other herbaceous vegetation (see Fig. 8) in Kyzyl-Orda.

6.2. Mapping abandoned cropland

In some regions of the world, e.g. in those characterized by intensive rain fed agriculture, fallow periods characterized by e.g. the absence of recognizable management can be a strong indicator for land abandonment (Stefanski et al., 2014a, b). The proposed LCT analysis, which includes several consecutive years, demonstrated

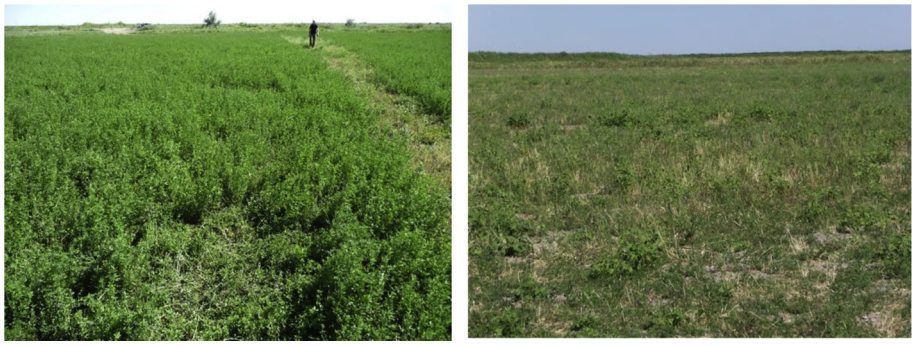

Fig. 8. Alfalfa field (left) and field with mixed herbaceous vegetation (right). Both fields have also been used for rice cultivation in rotation with a 2–3 years lasting fallow period.

that at best maps from several consecutive years are required for identifying abandoned cropland. This is due to habit in Kyzyl-Orda to fallow for several years between years of rice cultivation. Likewise, including all land use maps for 2009–2014 for the LCT analysis resulted in the highest overall accuracy for detection of agricultural land abandonment. Usually, cropland abandonment in Kyzyl-Orda results in a succession of weeds or grasses, and eventually the (re-) establishment of shrubs or trees. Vice versa, fallow lands that are characterized by herbaceous vegetation, partly even with sparse shrub cover could be part of a purposed crop rotation cycle (e.g. alfalfa periods as a means of soil conservation), making it difficult to ascertain whether or not a field has been truly abandoned and certainly when only one season/year is considered (Alcantara et al., 2012; Prishchepov et al., 2012a, b). With restricted observation lengths, the rather short rice cultivation periods in Kyzyl-Orda (1–2 years) could hardly be detected for every field, which in turn would lead to an ill-detection of abandoned cropland. Irrespectively of the absence of suitable images before 2000, which certainly has hampered the application of detailed LCT analysis for the Soviet Union period, the application of the bi-annual change detection for abandoned land detection as suggested by other authors (Prishchepov et al., 2012a, b) would most likely have led to reduced accuracies or even ill-detection of abandoned cropland. In this regard, the utilization of digitized field boundaries, which represent all ever-used field parcels, can be seen as a suitable workaround for bi-temporal change detection, even though the exact timing of cropland abandonment remains unknown. An alternative would be to digitize cadastre maps or Corona satellite images from the Soviet epoch. However such a map was unavailable for this study. As an alternative to field cadastres, a second analysis of LCT in Soviet times could be envisaged, given that suitable images are available, which was not the case in our study.

Despite the high accuracy of the method used, the status of almost 15% of the fields remained uncertain, i.e. these were characterized by not particularly investigated change classes, including implausible classes. This is most probably due to misclassifications that resulted in rather unlikely changes of, for instance, rice and shrubs. Such change classes were labelled “uncertain” because any assignment to abandoned or actively used fields dropped the accuracy of the method below its comparatively high level (not shown here). An interesting addition could be an investigation about the influence of classification uncertainty propagation in the land cover analysis and its impact on the reliability of the land abandonment detection (e.g. Cockx et al., 2014).

Furthermore, ca. 18% of the fields followed a rotation of herbaceous vegetation and shrubs. Although this was assigned as “abandoned fields”, the question remains why such a sequence of these land use classes occurred. One possible explanation may be that in years of increased water availability, which usually results in an overall elevation of ground water levels, the establishment of annual herbaceous vegetation on sparse shrublands was enhanced due to the high groundwater levels (Fig. 9). In any case, the sequence of both could have resulted in a mixed signal, which in turn hampered the separation of shrubs from herbaceous vegetation. The same could apply for combinations of soils and herbaceous vegetation, which covered ca 3% of the fields.

The accuracy of the proposed method to detect abandoned cropland (about 0.80) ranges among previously reported accuracies. For instance, Alcantara et al. (2012) achieved about 0.65 accuracy, and Prishchepov et al., 2012a, b achieved accuracies of 0.74–0.90 for specific classes related with land abandonment, based on classifications of MODIS and Landsat data, respectively. A combination of radar and optical data could further increase the accuracy, as was previously demonstrated by Stefanski et al. (2014a, b).

6.3. Spatial pattern of abandoned cropland

Previous research postulated that the process of irrigated area expansion during the Soviet period mostly followed the principle of using land according to the soil productivity. For instance, Edlinger, Conrad, Lamers, Khasankhanova, and Koellner (2012) showed at the example of the Karshi steppe in Uzbekistan that conversion of steppes to irrigated land followed a certain scheme, i.e. expansion of irrigation system always moved towards soil classes of highest quality, whilst *Takyric* soils were only included after all high level land was in use. Yet, the analysis of the observed pattern of cropland abandonment, the third objective, indicated that land abandonment in Kyzyl-Orda was only to a certain degree triggered by soil conditions. Since the *Takyric Yermosols* in Kyzyl-Orda are considered to be less suitable for cropping due to the low inherent fertility, high salinity, and low pH values (FAO-UNESCO, 1974; IUSS Working Group WRB, 2014), and one could have hypothesized that abandoned fields would have occurred first on these soils. However, this was not the case and approximately 23% of the actively used fields were located on *Eutric Histosols*. Land use planners may have prioritized exploiting these soils since the profitability of farming can be high once the soils are adequately drained and investments have been made. Similar comparisons of remotely sensed indicators for land abandonment and soil maps in the western part of the Ukraine showed comparable mismatches between the intensity of land use and the quality of soils (Stefanski et al. 2014a, b). In their study area, Stefanski et al. (2014a, b) found about 20% of the rather fertile *Phaeozems* or *Chernozems* used for pastures or even fallow.

Although identifying various drivers for cropland abandonment in Kyzyl-Orda went beyond the scope of this study, it is very likely that environmental and economic drivers are among them. For

Fig. 9. Abandoned fields, which are characterized by homogeneous shrub cover and bare soil (left) and a mix of herbaceous vegetation and shrubs with little bare soil cover (right).

instance, secondary salinization or water availability were reported important drivers from similar lowland irrigation systems in Uzbekistan (Conrad, Dech, Hafeez, Lamers, & Tischbein, 2013; Tischbein et al., 2013). Irrigation infrastructure, drainage capacities, or groundwater levels could be drivers for reduced land use in irrigated areas, as was recently shown by Fritsch, Conrad, Dürbeck, and Schorcht (2014). Moreover, the observed pattern of cropland abandonment often depicts consequences of the privatization of the agricultural sector in Kazakhstan after independence in 1991 (Anderson & Swinnen, 2008). Furthermore, the study region is located in a part of Kazakhstan with a strong focus on rice production and FAO statistics illustrate that rice production areas in Kazakhstan have dropped from about 110,000 ha to 65,000 ha in the period 1993–2002, but then increased to an average of 91,200 ha in the period 2009–2013 (http://faostat3.fao.org, last access 01-Mar 2015). This indicated that at least parts of the cultivated land identified in this study had already been re-cultivated during the past decade and that the previous decisions and production inputs of the landowners, e.g. during the privatization process, could have influenced as well the observed spatial land use patterns. Also, developments of the population and employment structures, which is likely affected by the decline in agriculture's economic importance in Kazakhstan due to a booming energy sector (Anderson & Swinnen, 2008), should be taken into account when looking for drivers of cropland abandonment.

For a better understanding of the timing of agricultural transformation processes in Kyzyl Orda (cultivation, abandonment, and re-cultivation), bi- or multi-temporal mapping as applied by Stefanski et al. (2014) and Prishchepov et al. (2012a, b) could be considered in future investigations. However, such comparisons only highlight a single year within a multi-year crop rotation, which in turn would lead to reduced accuracy in comparison to multi-year trajectories covering the entire rotation scheme as shown in this study. Although a comparison of two several-years-lasting periods in Soviet and post-Soviet times would be beneficial, such an analysis was prohibitive due to the unavailability of images spanning such a suitable period in the Soviet times.

7. Conclusions

Abandoned cropland was mapped in an irrigated agricultural region in Kyzyl-Orda, southern Kazakhstan, which is predominated by rice cultivation. An object-based decision fusion approach was designed to create annual maps of agricultural land use during 2009–2014. The fusion of the results from RF and SVM classifiers resulted in significantly higher classification accuracies than the single algorithms. This underlined the value of the fusion approach for complex land use mapping.

The results showed that the use of satellite remote sensing for LCT analysis, based on the field boundaries of all ever-cultivated agricultural fields, was a suitable means to characterize the land use intensity and to detect abandoned cropland with an accuracy of almost 84%. The accuracy was increasing with the length of the trajectory, i.e. with an increasing number of land use maps from consecutive years. It was demonstrated that LCT analysis in perennial rotation systems, which include crops that are spectrally similar to natural herbaceous vegetation on abandoned land, requires at best gapless and consecutive multi-annual observations to avoid misinterpretation of land use trajectories and to reduce unexplainable area portions.

Based on the encroachment of shrubs, abandoned cropland was found on almost 50% of the fields in the study region. The remaining uncertainties on ca. 15% of the fields could eased in future through the use of hyperspectral and SAR data. Reasons for the widespread cropland abandonment in Kyzyl-Orda might be numerous and further research could focus on assessing the driving factors of cropland abandonment.

Overall, the presented approach constitutes a very accurate means to map agricultural land use and identify abandoned cropland over large areas where a complex crop rotation pattern prevails. It contributes to a better understanding of land abandonment processes in Kyzyl-Orda, but could also be tested in other regions across Central Asia. The outcomes may assist researchers, planners, policy- and decision-makers to better monitor cropland abandonment. The use of satellite EO enables collecting important information at the regional scale, which could be used for supporting better-informed decisions to reduce possible environmental impacts of cropland abandonment, for instance by identifying areas that could be targeted for alternative land uses like pasture, or re-cultivation.

Acknowledgements

This work was undertaken at the University of Würzburg, Department of Remote Sensing, within the CAWa project funded by the German Federal Foreign Office, and the project “LaVaCCA”, funded by the Volkswagen foundation. We thank the German Aerospace Agency (DLR) for providing data from the RapidEye Science Archive (RESA). The German National Academic Foundation (Az: 88506) funded this research by way of a PhD grant to the first author. The authors would like to thank the Deutsche Gesellschaft für Internationale Zusammenarbeit (GIZ) for supporting the field studies in Kyzyl-Orda. The authors would also like to thank the anonymous reviewers for their valuable comments.

References

Akramkhanov, A., & Vlek, P. L. G. (2012). The assessment of spatial distribution of soil salinity risk using neural network. *Environmental. Monitoring. Assessment, 184*, 2475–2485.

Alcantara, C., Kuemmerle, T., Prishchepov, A. V., & Radeloff, V. C. (2012). Mapping abandoned agriculture with multi-temporal MODIS satellite data. *Remote Sensing of Environment, 124*, 334–347. http://dx.doi.org/10.1016/j.rse.2012.05.019.

Anderson, K., & Swinnen, J. (2008). *Distortions to agricultural incentives in Europe's transition economies*. Washington, DC: The world bank.

Baumann, M., Kuemmerle, T., Elbakidze, M., Ozdogan, M., Radeloff, V. C., Keuler, N. S., et al. (2011). Patterns and drivers of post-socialist farmland abandonment in Western Ukraine. *Land use policy, 28*, 552–562. http://dx.doi.org/10.1016/j.landusepol.2010.11.003.

Beurs, K. de (2004). Trend analysis of the pathfinder AVHRR land (PAL) NDVI data for the deserts of Central Asia. *Geoscience and Remote Sensing, 1*, 282–286.

Blaschke, T. (2010). Object based image analysis for remote sensing. *ISPRS Journal of Photogrammetry and Remote Sensing, 65*, 2–16. http://dx.doi.org/10.1016/j.isprsjprs.2009.06.004.

Breiman, L. (2001). Random forests. *Machine Learning, 45*, 5–32.

Breiman, L., & Cutler, A. (2007). *Random forests — Classification description: Random forests* [WWW Document]. stat www.berkeley.edu/users/breiman/RandomForests/cc_home.htm Accessed 01.11.13.

Burges, C. J. C. (1998). A tutorial on support vector machines for pattern recognition. *Data Mining and Knowledge Discovery, 2*, 121–167.

Burnicki, A. C., Brown, D. G., & Goovaerts, P. (2007). Simulating error propagation in land-cover change analysis: the implications of temporal dependence. *Computers, Environment and Urban Systems, 31*, 282–302. http://dx.doi.org/10.1016/j.compenvurbsys.2006.07.005.

Cockx, K., Van de Voorde, T., & Canters, F. (2014). Quantifying uncertainty in remote sensing-based urban land-use mapping. *International Journal Applied Earth Observation and Geoinformation, 31*, 154–166. http://dx.doi.org/10.1016/j.jag.2014.03.016.

Congalton, R. G. (1991). A review of assessing the accuracy of classifications of remotely sensed data. *Remote Sensing of Environment, 37*, 35–46.

Conrad, C., Dech, S., Dubovyk, O., Fritsch, S., Klein, D., Löw, F., et al. (2014). Derivation of temporal windows for accurate crop discrimination in heterogeneous croplands of Uzbekistan using multitemporal RapidEye images. *Computers and Electronics in Agriculture, 103*, 63–74.

Conrad, C., Dech, S. W., Hafeez, M., Lamers, J. P. a., & Tischbein, B. (2013). Remote sensing and hydrological measurement based irrigation performance assessments in the upper amu darya Delta, Central Asia. *Physics and Chemistry of the Earth, Parts A/B/C, 61–62*, 52–62. http://dx.doi.org/10.1016/j.pce.2013.05.002.

Cortes, C., & Vapnik, V. (1995). Support-vector networks. *Machine Learning, 20*, 273–297.

De Beurs, K. M., Henebry, G. M., & Debeurs, K. (2004). Land surface phenology, climatic variation, and institutional change: analyzing agricultural land cover change in Kazakhstan. *Remote Sensing of Environment, 89*, 497–509. http://dx.doi.org/10.1016/j.rse.2003.11.006.

De Beurs, K. M., Wright, C. K., & Henebry, G. M. (2009). Dual scale trend analysis for evaluating climatic and anthropogenic effects on the vegetated land surface in Russia and Kazakhstan. *Environmental Research Letters, 4*, 045012. http://dx.doi.org/10.1088/1748-9326/4/4/045012.

De Wit, A., & Clevers, J. G. P. W. (2004). Efficiency and accuracy of per-field classification for operational crop mapping. *International Journal of Remote Sensing, 25*(20), 4091–4112. http://dx.doi.org/10.1080/01431160310001619580.

Dregne, H. E. (2002). Land degradation in the drylands. *Arid Land Research and Management, 16*, 99–132.

Duveiller, G., & Defourny, P. (2010). A conceptual framework to define the spatial resolution requirements for agricultural monitoring using remote sensing. *Remote Sensing of Environment, 114*, 2637–2650. http://dx.doi.org/10.1016/j.rse.2010.06.001.

Edlinger, J., Conrad, C., Lamers, J. P. A., Khasankhanova, G., & Koellner, T. (2012). Reconstructing the spatio-temporal development of irrigation systems in Uzbekistan using landsat time series. *Remote Sensing, 4*, 3972–3994. http://dx.doi.org/10.3390/rs4123972.

Estel, S., Kuemmerle, T., Alcantara, C., Levers, C., Prishchepov, a. V., & Hostert, P. (2015). Mapping farmland abandonment and recultivation across Europe using MODIS NDVI time series. *Remote Sensing of Environment*. http://dx.doi.org/10.1016/j.rse.2015.03.028.

Falcucci, A., Maiorano, L., & Boitani, L. (2006). Changes in land-use/land-cover patterns in Italy and their implications for biodiversity conservation. *Landscape Ecology, 22*, 617–631. http://dx.doi.org/10.1007/s10980-006-9056-4.

FAO. (2015). *Food and agriculture organization of the united nations (FAOSTAT)* [WWW Document]. URL http://faostat3.fao.org/faostat-gateway/go/to/home/E http://faostat3.fao.org/faostat-gateway/go/to/home/E.

FAO-UNESCO. (1974). *Soil map of the world*. Paris: FAO, ISBN 92-3-101125-1.

Fauvel, M., Chanussot, J., & Benediktsson, J. A. (2006). Decision fusion for the classification of urban remote sensing images. *IEEE Transactions on Geoscience and Remote Sensing*, 2494–2497. http://dx.doi.org/10.1109/IGARSS.2006.645.

Fliemann, E., Löw, F., & Conrad, C. (2014). Assessing the potential of landsat images to detect and map agricultural land abandonment in Kyzyl-Orda (Kazakhstan). *Geophysical Research Abstracts, 16*.

Foley, J. A., Ramankutty, N., Brauman, K. a, Cassidy, E. S., Gerber, J. S., Johnston, M., et al. (2011). Solutions for a cultivated planet. *Nature, 478*, 337–342. http://dx.doi.org/10.1038/nature10452.

Foody, G. M. (2009). Classification accuracy comparison: hypothesis tests and the use of confidence intervals in evaluations of difference, equivalence and non-inferiority. *Remote Sensing of Environment, 113*, 1658–1663. http://dx.doi.org/10.1016/j.rse.2009.03.014.

Foody, G. M. (2010). Assessing the accuracy of land cover change with imperfect ground reference data. *Remote Sensing of Environment, 2285*, 2271–2285.

Foody, G. M., Boyd, D. S., & Sanchez-Hernandez, C. (2007). Mapping a specific class with an ensemble of classifiers. *International Journal of Remote Sensing, 28*, 1733–1746.

Fritsch, S., Conrad, C., Dürbeck, T., & Schorcht, G. (2014). Mapping marginal land in khorezm using GIS and remote sensing techniques. In J. P. A. Lamers, A. Khamzina, I. Rudenko, & P. L. G. Vlek (Eds.), *Restructuring land allocation, water use and agricultural value chains. Technologies, policies and practices for the lower amudarya region* (pp. 167–178). Goettingen: V & R unipress. Bonn University Press.

Funakawa, S., Suzuki, R., Karbozova, E., Kosaki, T., & Ishida, N. (2000). Salt-affected soils under rice-based irrigation agriculture in southern Kazakhstan. *Geoderma, 97*, 61–85.

Giacco, F., Thiel, C., Pugliese, L., Scarpetta, S., & Marinaro, M. (2010). Uncertainty analysis for the classification of multispectral satellite images using SVMs and SOMs. *IEEE Transactions on Geoscience and Remote Sensing, 48*, 3769–3779.

Gislason, P., Benediktsson, J. A., & Sveinsson, J. R. (2006). Random forests for land cover classification. *Pattern Recognition Letters, 27*, 294–300.

Glantz, M. H. (2009). *Creeping environmental problems and sustainable development in the aral sea Basin*. Cambridge: Cambridge University Press.

Ho, T. K. (1998). The random subspace method for constructing decision forests. *IEEE Transactions on Pattern Analysis.and Machine Intelligence, 20*, 823–844.

Huang, C., Davis, L. S., & Townshend, J. R. G. (2002). An assessment of support vector machines for land cover classification. *International Journal of Remote Sensing, 23*, 725–749. http://dx.doi.org/10.1080/01431160110040323.

Huang, C., Wylie, B., Yang, L., Homer, C., & Zylstra, G. (2002). Derivation of a tasselled cap transformation based on landsat 7 at-satellite reflectance. *International Journal of Remote Sensing, 23*, 1741–1748. http://dx.doi.org/10.1080/01431160110106113.

Huete, A., Didan, K., Miura, T., Gao, X., & Ferreira, L. G. (2002). Overview of the radiometric and biophysical performance of the MODIS vegetation indices. *Remote Sensing of Environment, 83*, 195–213.

Ibraeva, M. A., Otarov, A., Wiłkomirski, B., & Suska-malawska, M. (2010). HUMUS level IN soils of southern kazakhstan irrigated massifs and their statistical characteristics. *Monit. Środowiska Przyr, 11*, 55–61.

IUSS Working Group WRB. (2014). *World reference base for soil resources 2014* (Rome).

Jeon, B., & Landgrebe, D. A. (1999). Decision fusion approach for multitemporal classification. *IEEE Transactions on Geoscience and Remote Sensing, 37*, 1227–1233.

Kauth, R. J., & Thomas, G. S. (1976). The tasselled cap – a graphic description of the spectral-temporal development of agricultural crops as seen by landsat. In *Proceedings of symposium on machine processing of remotely sensed data*. West Layette: Purdue University, 4B-41–4B-51.

Kuemmerle, T., Erb, K., Meyfroidt, P., Müller, D., Verburg, P. H., Estel, S., et al. (2013). Challenges and opportunities in mapping land use intensity globally. *Current Opinion.in Environmental Sustainability, 5*, 484–493. http://dx.doi.org/10.1016/j.cosust.2013.06.002.

Kuemmerle, T., & Griffiths, P. (2009). Land use change in southern Romania after the collapse of socialism. *Regional Environmental Change, 9*.

Kuemmerle, T., Hostert, P., Radeloff, V. C., Linden, S., Perzanowski, K., & Kruhlov, I. (2008). Cross-border comparison of post-socialist farmland abandonment in the carpathians. *Ecosystems, 11*, 614–628. http://dx.doi.org/10.1007/s10021-008-9146-z.

Lambin, E. F., & Geist, H. J. (2006). *Land-use and land-cover change: Local process- es and global impacts, change*. Berlin, Heidelberg, New York: Springer.

Lambin, E. F., & Meyfroidt, P. (2011). Global land use change, economic globalization, and the looming land scarcity. *PNAS, 108*, 3465–3472.

Létolle, R., & Mainguet, M. (1996). *Der Aralsee: eine ökologische Katastrophe*. Berlin, Heidelberg, New York: Springer.

Licciardi, G., Pacifici, F., Tuia, D., Prasad, S., West, T., Giacco, F., et al. (2009). Decision fusion for the classification of hyperspectral data: outcome of the 2008 GRS-S data fusion contest. *IEEE Transactions on Geoscience and Remote Sensing, 47*, 3857–3865.

Loosvelt, L., Peters, J., & Skriver, H. (2012). Impact of reducing polarimetric SAR input on the uncertainty of crop classifications based on the random forests algorithm. *IEEE Transactions on Geoscience and Remote Sensing, 50*, 4185–4200.

Löw, F., & Duveiller, G. (2014). Defining the spatial resolution requirements for crop identification using optical remote sensing. *Remote Sensing, 6*, 9034–9063. http://dx.doi.org/10.3390/rs6099034.

Löw, F., Michel, U., Dech, S., & Conrad, C. (2013). Impact of feature selection on the accuracy and spatial uncertainty of per-field crop classification using support vector machines. *ISPRS Journal of Photogrammetry and Remote Sensing, 85*, 102–119. http://dx.doi.org/10.1016/j.isprsjprs.2013.08.007.

Martinez-Casasnovas, J., Martín-Montero, A., & Auxiliadora Casterad, M. (2005). Mapping multi-year cropping patterns in small irrigation districts from time-series analysis of landsat TM images. *European Journalof Agronomy, 23*, 159–169. http://dx.doi.org/10.1016/j.eja.2004.11.004.

Mountrakis, G., Im, J., & Ogole, C. (2011). Support vector machines in remote sensing: a review. *ISPRS Journal of Photogrammetry and Remote Sensing, 66*, 247–259. http://dx.doi.org/10.1016/j.isprsjprs.2010.11.001.

Müller, D., Kuemmerle, T., Rusu, M., & Griffiths, P. (2009). Lost in transition: determinants of post-socialist cropland abandonment in Romania. *Journal of Land*

Use Science, 4, 109–129. http://dx.doi.org/10.1080/17474230802645881.
Murakami, T., Ogawa, S., Ishitsuka, N., Kumagai, K., & Saito, G. (2001). Crop discrimination with multitemporal SPOT/HRV data in the Saga Plains, Japan. *International Journal of Remote Sensing, 22*(7), 1335–1348. http://dx.doi.org/10.1080/01431160151144378.
Ozdogan, M., & Woodcock, C. E. (2006). Resolution dependent errors in remote sensing of cultivated areas. *Remote Sensing of Environment, 103*, 203–217. http://dx.doi.org/10.1016/j.rse.2006.04.004.
Pal, M. (2005). Random forest classifier for remote sensing classification. *International Journal of Remote Sensing, 26*, 217–222.
Pal, M., & Foody, G. M. (2010). Feature selection for classification of hyperspectral data by SVM. *IEEE Transactions on Geoscience and Remote Sensing, 48*, 2297–2307. http://dx.doi.org/10.1109/TGRS.2009.2039484.
Pal, M., & Mather, P. M. (2005). Support vector machines for classification in remote sensing. *International Journal of Remote Sensing, 26*, 1007–1011.
Park, S., & Egbert, S. L. (2008). Remote sensing-measured impacts of the conservation Reserve program (CRP) on landscape structure in southwestern Kansas. *GIScience & Remote Sensing, 45*, 83–108.
Peterson, U., & Aunap, R. (1998). Changes in agricultural land use in Estonia in the 1990s detected with multitemporal landsat MSS imagery. *Landscape and Urban Planning, 41*, 193–201. http://dx.doi.org/10.1016/S0169-2046(98)00058-9.
Power, A. G. (2010). *Ecosystem services and agriculture–: Tradeoffs and synergies ecosystem services and agriculture–: Tradeoffs and synergies*. Society (pp. 2959–2971). http://dx.doi.org/10.1098/rstb.2010.0143.
Prishchepov, A. V., Radeloff, V. C., Dubinin, M., & Alcantara, C. (2012). The effect of landsat ETM/ETM+ image acquisition dates on the detection of agricultural land abandonment in Eastern Europe. *Remote Sensing of Environment, 126*, 195–209. http://dx.doi.org/10.1016/j.rse.2012.08.017.
Prishchepov, A. V., Radeloff, V. C., Dubinin, M., & Alcantara, C. (2012). The effect of landsat ETM/ETM+ image acquisition dates on the detection of agricultural land abandonment in Eastern Europe. *Remote Sensing of Environment, 126*, 195–209. http://dx.doi.org/10.1016/j.rse.2012.08.017.
R Development Core Team. (2014). *A language and environment for statistical computing*.
Richter, R. (2011). *Atmospheric/Topographic correction for satellite imagery. ATCOR-2/3 user guide 7.1* (Wessling).
Rouse, J. W., Haas, R. H., Schell, J. A., & Deering, D. W. (1974). Monitoring vegetation systems in the great Plains with ERTS. In S. C. Freden, E. P. Mercanti, & M. A. Becker (Eds.), *Proceedings of the earth resources technology satellite symposium NASA SP-351* (pp. 309–317). Washington, DC: NASA.
Schönert, M., Weichelt, H., Zillmann, E., & Jürgens, C. (2014). Derivation of tasseled cap coefficients for RapidEye data. In U. Michel, & K. Schulz (Eds.), *Earth resources and environmental remote Sensing/GIS applications* (Vol. 9245, p. 92450Q). SPIE. http://dx.doi.org/10.1117/12.2066842.
Schuster, C., Ali, I., Lohmann, P., Frick, A., & Förster, M. (2011). Towards detecting swath events in TerraSAR-X time series to Establish NATURA 2000 grassland habitat swath management as monitoring parameter. *Remote Sensing, 3*, 1308–1322. http://dx.doi.org/10.3390/rs3071308.
Stefanski, J., Chaskovskyy, O., & Waske, B. (2014). Mapping and monitoring of land use changes in post-Soviet western Ukraine using remote sensing data. *Applied Geography, 55*, 155–164. http://dx.doi.org/10.1016/j.apgeog.2014.08.003.
Stefanski, J., Kuemmerle, T., Chaskovskyy, O., Griffiths, P., Havryluk, V., Knorn, J., et al. (2014). Mapping land management regimes in western Ukraine using optical and SAR data. *Remote Sensing, 6*, 5279–5305. http://dx.doi.org/10.3390/rs6065279.
Tischbein, B., Manschadi, A. M., Conrad, C., Hornidge, A., Bhaduri, A., Hassan, M. U., et al. (2013). Adapting to water scarcity: constraints and opportunities for improving irrigation management in Khorezm, Uzbekistan. *Water Science and Technology Water Supply*, 337–348. http://dx.doi.org/10.2166/ws.2013.028.
Verburg, P., Schot, P., Dijst, M., & Veldkamp, a (2004). Land use change modelling: current practice and research priorities. *GeoJournal, 61*, 309–324. http://dx.doi.org/10.1007/s10708-004-4946-y.
Wardlow, B. D., & Egbert, S.. L. (2008). Large-area crop mapping using time-series MODIS 250 m NDVI data: an assessment for the U.S. Central great Plains. *Remote Sensing of Environment, 112*, 1096–1116. http://dx.doi.org/10.1016/j.rse.2007.07.019.
Waske, B., & Braun, M. (2009). Classifier ensembles for land cover mapping using multitemporal SAR imagery. *ISPRS Journal of Photogrammetry and Remote Sensing, 64*, 450–457. http://dx.doi.org/10.1016/j.isprsjprs.2009.01.003.
Waske, B., & van der Linden, S. (2008). Classifying multilevel imagery from SAR and optical sensors by decision fusion. *IEEE Transactions on Geoscience and Remote Sensing, 46*, 1457–1466.
Waske, B., van der Linden, S., Benediktsson, J. A., Rabe, A., & Hostert, P. (2010). Sensitivity of support vector machines to random feature selection in classification of hyperspectral data. *IEEE Transactions on Geoscience and Remote Sensing, 48*, 2880–2889.
Wright, C. K., de Beurs, K. M., & Henebry, G. M. (2012). Combined analysis of land cover change and NDVI trends in the Northern Eurasian grain belt. *Frontiers of Earth Science, 6*, 177–187.